Research Report

2001-04

Electromagnetic Vibration and Noise Assessment for Surface Mounted PM Machines

S. Huang*, M. Aydin, T.A. Lipo

* Department of Automation
Shanghai University
149 Yan-Chang Road
Shanghai, 200072, P.R. China

Wisconsin Power Electronic
Research Center
University of Wisconsin - Madison
Madison, WI 53706

Wisconsin
Electric
Machines &
Power
Electronics
Consortium

University of Wisconsin-Madison
College of Engineering
Wisconsin Power Electronics Research Center
2559D Engineering Hall
1415 Engineering Drive
Madison WI 53706-1691

Power Engineering Society Summer Meeting, 2001

Electromagnetic Vibration and Noise Assessment for Surface Mounted PM Machines

S. Huang*, M. Aydin**, Student Member, IEEE T. A. Lipo**, Fellow, IEEE

* Department of Automation
Shanghai University
149 Yan-Chang Road
Shanghai, 200072, P.R.China

** Department of Electrical and Computer Engineering
University of Wisconsin-Madison
1415 Engineering Drive
Madison, WI 53706-1691, USA

Abstract: Analysis of electromagnetic vibration and acoustic noise assessment and methods to minimize resultant sound power level for low noise motor design is presented in this paper. The linear model of the exciting force wave is derived to evaluate the exciting force and to optimize the design of stator winding, rotor PM shape and rotor PM skew angle for minimization of resultant sound power level for low noise motor design. Mode number and frequency of the exciting force wave, natural vibration frequency, maximum vibration velocity and maximum vibration displacement of main vibration source are introduced to evaluate machine vibration. Resultant sound power levels for the cylindrical sound wave and the plane sound wave models are introduced to analyze the acoustic noise assessment of both axial and radial flux PM machines respectively. Finally, electromagnetic vibration and acoustic noise assessment of both radial and axial flux surface mounted motor structures are completed and illustrated in the paper.
Keywords: Vibration, Acoustic noise, Exciting force wave, Surface mounted PM machines

I. NOMENCLATURE

$b(\theta,t)$	air gap flux density waves
μ_0	permeability of free space
θ	space coordinate in radians around the circumference of air gap surface
$f(\theta,t)$	air gap MMF
$\Lambda(\theta)$	air gap permeance
μ	order of the space harmonic for the excitation field
ν	order of the space harmonic for the armature field
ω_1	fundamental angular frequency
p	fundamental pole pair for the excitation MMF
B_μ	μ^{th} space harmonic of the air gap flux density for the excitation field
δ_g	physical air gap length
$\overline{\Lambda}_0$	mean air gap permeance in per unit
$\overline{\Lambda}_k$	k^{th} slotting permeance in per unit
Z_s	number of the stator slots
k	order of the stator slot permeance
K_{cs}	Carter factor for the stator slotting
K_{f_μ}	form factor of the μ^{th} space harmonics
K_{os_μ}	open slot factor of the μ^{th} space harmonics
K_{s_μ}	skew factor of the μ^{th} space harmonics
B_g	amplitude of the airgap flux density for the excitation field
α_i	pole arc ratio for PM rotor
α_{skew}	skew angle
ψ	phase angle of the fundamental EMF
B_ν	ν^{th} space harmonics for the armature field
$K_{w\nu}$	winding factor of the ν^{th} space harmonics
K_{w1}	winding factor of the fundamentals
$\overline{X}_{ad}$	armature reactance in d axis in per unit
Y_{pk-r}	amplitude of the particle vibratory displacement
ρ	density of the medium
f_r	frequency of the sound wave
C	traveling speed of sound in the medium
S_{Cylin}	surface vibration area for the radial flux cylindrical machine
I_{re-r}	relative sound intensity coefficient
S_{Plane}	surface vibration area for the axial flux disc machines
W_i	sound power
$W_0 = 10^{-12}\,[w]$	reference value of the sound power

*Surong Huang was supported by Wisconsin Power Electronics Research Center and Chinese National Science Foundation (59877014).

II. INTRODUCTION

In practice, evaluation of different machine types is a very formidable task. However, a systematic method to evaluate the electrical machines performance with different topologies has been established [1-2]. First, the generalized sizing equations are used to evaluate different radial and axial flux surface mounted permanent magnet (PM) machines and optimize main size in terms of torque/power densities, efficiencies, utilization, heat dissipation and weight [3]. Second, the general instantaneous electromagnetic torque equation and torque ripple factor (TRF) depending on harmonic components of winding distribution, airgap field distribution, rotor magnet skew angle and open slot effect are used to evaluate torque quality and optimum design for minimum ripple and maximum torque density [4]. Next, the liner model of exciting force wave, the vibration displacement model, the sound power for the cylindrical sound wave and the plane sound wave models will be introduced in this paper in order to evaluate the electromagnetic vibration and acoustic noise assessment of the surface mounted PM machines.

mechanical and acoustic analysis and calculation of the electrical machines rather than focusing on electromagnetic design. The existing research on vibration and acoustic noise can be mainly divided into two methods: the frequency domain method and the time domain method. The frequency domain method, which can be developed using sizing equations, can be used to predict the spectrum and dominant components of the noise and vibration as well as the natural frequencies in terms of machine geometry and elasticity modulus of the machine components. In addition, time domain methods can be developed using Finite Element Software.

In this paper, for the purpose of the evaluation of the exciting force, the linear model of the exciting force wave for surface mounted PM machines based on the liner model of the air gap resultant field and the air gap permeance wave is derived. Mode number and frequency of the exciting force wave, nature vibration frequency concentrating on the natural vibration modes of the machine components, vibration displacement of the machine of the mode number and frequency concerned, equivalent exciting force in the airgap surface for the mode number and frequency concerned are introduced in order to evaluate machine vibration. Moreover, the sound power for the cylindrical sound wave model and for the plane sound wave model are introduced in order to evaluate the acoustic noise assessment of both axial flux and radial flux surface mounted PM machines respectively.

Based on the linear model of the exciting force wave analysis, optimum design for stator winding, PM rotor shape and PM rotor skew angle can be achieved for minimization of sound power level for low noise motor design. Finally, electromagnetic vibration and acoustic noise assessment of both axial flux and radial flux surface mounted motor structures (Torus, single rotor axial flux and conventional radial flux machines) are completed and illustrated in the paper.

III. LINEAR MODEL OF EXCITING FORCE WAVE

According to Maxwell's equations, the exciting force wave is proportional to the square of the normal component of the air gap flux density

$$p_{ef}(\theta,t) = \left\{ \frac{b^2(\theta,t)}{2\mu_0} \quad \begin{array}{l} \text{In the radial direction for radial flux topologies} \\ \text{In the axial direction for the axial flux topologies} \end{array} \right. \quad (1)$$

where $b(\theta,t)$ is the air gap flux density waves, μ_0 is the permeability of free space, θ is the space coordinate in radians around the circumference of air gap surface, t is the time.

In general, the air gap flux density can be expressed as the product of the air gap MMF and the air gap permeance. The airgap MMF is composed of the excitation MMF of the rotor PM and the armature MMF of the stator winding. For PM machines,

$$b(\theta,t) = f(\theta,t)\,\Lambda(\theta) = \left[\sum_{\mu} f_{\mu}(\theta,t) + \sum_{\nu} f_{\nu}(\theta,t) \right] \Lambda(\theta) \quad (2)$$

where $f(\theta,t)$ is the air gap MMF, $\Lambda(\theta)$ is the air gap permeance, $\sum_{\mu} f_{\mu}(\theta,t)$ is the excitation MMF of rotor PM, $\sum_{\nu} f_{\nu}(\theta,t)$ is the armature MMF of stator winding, μ is the order of the space harmonic for the excitation field, and ν is the order of the space harmonic for the armature field.

Neglecting the saturation effects for the development of an algorithm for computation and using the principle of the flux superposition, the air gap flux density is composed of the excitation field of the rotor PM and the armature field of the stator winding. The linear model of the air gap resultant field can be written as

$$\begin{aligned} b(\theta,t) &= b_{ex}(\theta,t) + b_{ar}(\theta,t) \\ &= \sum_{\mu} f_{\mu}(\theta,t)\ \Lambda(\theta) + \sum_{\nu} f_{\nu}(\theta,t)\ \Lambda(\theta) \end{aligned} \quad (3)$$

where $b_{ex}(\theta,t)$ is the excitation field waves of the rotor PM, and $b_{ar}(\theta,t)$ is the armature field waves of the stator winding.

The μ^{th} space harmonic of the excitation MMF for the surface mounted PM machine is given by

$$f_{\mu}(\theta,t) = B_{\mu} \frac{\delta_g}{\mu_0} \cos(\mu\omega_1 t - \mu p \theta) \quad (4)$$

where ω_1 is the fundamental angular frequency, p is the fundamental pole pair for the excitation MMF, B_{μ} is the μ^{th} space harmonic of the air gap flux density for the excitation field, δ_g is the physical air gap length. The order of the space harmonic for the excitation field is

$$\mu = (2n+1) \quad (5)$$

where $n = 0, 1, 2, 3, \ldots$

The air gap permeance represents almost the total permeance of the magnetic circuit. Slotting breaks up the uniformity of the air gap and produces the periodical variation and a strong harmonic content in the air gap permeance wave.

In reality eccentricity of the rotor and iron saturation gives rise to more distorted air gap permeance wave. In order to simplify the formula of the air gap permeance wave for the surface mounted PM machine, the effects of the eccentricity and saturation will be neglected. In this case, the air gap permeance wave only consists of the effect of the stator slotting and mean air gap which can be expressed as [1, 5]

$$\Lambda(\theta)=\frac{\mu_0}{\delta_g}\left[\overline{\Lambda}_0+\sum_{k=1}^{\infty}(-1)^{k+1}\overline{\Lambda}_k\cos(kZ_s\theta)\right] \quad (6)$$

where $\overline{\Lambda}_0$ is the mean air gap permeance in per unit, $\overline{\Lambda}_k$ is the k^{th} slotting permeance in per unit, Z_s is the number of the stator slots, k is the order of the stator slot permeance. The mean permeance can be calculated as

$$\overline{\Lambda}_0=\frac{1}{K_{cs}}\leq 1 \quad (7)$$

and the k^{th} slotting permeance in per unit is defined as

$$\overline{\Lambda}_k=\frac{K_{cs}-1}{K_{cs}}\left|\frac{\sin(k\frac{K_{cs}-1}{K_{cs}}\pi)}{k\frac{K_{cs}-1}{K_{cs}}\pi}\right| \quad (8)$$

where K_{cs} is the Carter factor for the stator slotting.

Inserting Equations (4) and (6) into (3), the excitation field model for the surface mounted PM machine becomes

$$b_{ex}(\theta,t)=\sum_{\mu}(B_\mu\overline{\Lambda}_0\cos(\mu\omega_1 t-\mu p\theta)$$
$$+\sum_{\mu}\sum_{k}(-1)^{k+1}\frac{B_\mu\overline{\Lambda}_k}{2}\cos\left[\mu\omega_1 t-(\mu p\pm kZ_s)\theta\right] \quad (9)$$

In Equation (9), the first term is the main pole field of the excitation field considering the fact that the mean air gap permeance is reduced by slotting. The second term is the additional field of slotting permeance. The air gap permeance produces periodical variation with slotting, and this additional field will interfere the main pole field.

The amplitude of the μ^{th} space harmonic for the excitation field is

$$B_\mu=K_{f\mu}K_{os\mu}K_{s\mu}B_g \quad (10)$$

where K_{f_μ} is the form factor of the μ^{th} space harmonics, K_{os_μ} is the open slot factor of the μ^{th} space harmonics, K_{s_μ} is the skew factor of the μ^{th} space harmonics, and B_g is the amplitude of the airgap flux density for the excitation field. In the surface mounted PM machine, the excitation field has a quasi-rectangular waveform. Using Fourier analysis, the μ^{th} form factor of the excitation field is found to be

$$K_{f\mu}=\frac{4}{\mu\pi}\sin\frac{\mu\alpha_i\pi}{2} \quad (11)$$

where $\alpha_i=W_{PM}/\tau_P$ is the pole arc ratio for PM rotor. In the slotted topology, it is well known that skewing can reduce the slot harmonics. The μ^{th} harmonic skew factor can be expressed as

$$K_{s\mu}=\frac{\sin(\mu\frac{\alpha_{skew}}{2})}{\mu\frac{\alpha_{skew}}{2}} \quad (12)$$

where α_{skew} is the skew angle. The open slot factor of the μ^{th} space harmonic is derived as [1,4]

$$K_{os_\mu}=1-\sum_{k=1}^{\infty}\left(\frac{\overline{\Lambda}_k}{\overline{\Lambda}_0}\frac{\mu^2}{\mu^2-(\frac{kZ_s}{p})^2}\right) \quad (13)$$

From AC machine principles, the armature field can be written as [5]

$$b_{ar}(\theta,t)=\sum_{\nu}f_\nu(\theta,t)\,\Lambda(\theta)$$
$$=\sum_{\nu}B_\nu\cos\left[\omega_1 t-\nu p\theta-(\psi+\frac{\pi}{2})\right] \quad (14)$$

where ψ is the phase angle of the fundamental EMF leading the fundamental current and B_ν is the ν^{th} space harmonics for the armature field. The order of the space harmonics for the armature field is

$$\nu=2m_1q'+1 \quad (15)$$

where $q'=0,\ \pm1,\ \pm2,\ \cdots$.

When $q'=\pm q_s,\ \pm 2q_s,\ \pm 3q_s,\ \cdots$, the order of the slot winding harmonic of the armature field can be written as

$$\nu_z=\mp k\frac{Z_s}{p}+1 \quad (16)$$

The amplitude of the ν^{th} space harmonic of the armature field is [6]

$$B_\nu = \frac{1}{\nu} \left| \frac{K_{w\nu}}{K_{w1}} \right| \overline{X}_{ad}\ B_g \tag{17}$$

where K_{w_ν} is the winding factor of the ν^{th} space harmonics, K_{w1} is the winding factor of the fundamentals, $\overline{X}_{ad}$ is the per unit of the armature reactance in d-axis.

Inserting Equations (9) and (14) into (3), the air gap resultant field model for the surface mounted PM machine becomes

$$b(\theta,t) = \sum_{\mu} B_\mu\ \overline{\Lambda}_0 \cos(\mu\omega_1 t - \mu p\theta) + \sum_{\mu}\sum_{k} (-1)^{k+1} \frac{B_\mu \overline{\Lambda}_k}{2} \cos\left[\mu\omega_1 t - (\mu p \pm kZ_s)\,\theta\right] + \sum_{\nu} B_\nu \cos\left[\omega_1 t - \nu p\theta - (\psi + \frac{\pi}{2})\right] \tag{18}$$

Combining Equations (1) and (18), the linear model of exciting force wave for the surface mounted PM machine is expressed as

$$p_{ef}(\theta,t) = \frac{1}{2\mu_0}\Big\{ \sum_{\mu} B_\mu\ \overline{\Lambda}_0 \cos(\mu\omega_1 t - \mu p\theta) + \sum_{\mu}\sum_{k} (-1)^{k+1} \frac{B_\mu \overline{\Lambda}_k}{2} \cos\left[\mu\omega_1 t - (\mu p \pm kZ_s)\,\theta\right] + \sum_{\nu} B_\nu \cos\left[\omega_1 t - \nu p\theta - (\psi + \frac{\pi}{2})\right] \Big\}^2 \tag{19}$$

The constant components of the exciting force wave make the stator core to static distortion and cannot produce vibration and noise. Hence they will be neglected. In this case, the linear model of exciting force wave only comprises nine groups of infinite numbers of the exciting force wave, their amplitudes, mode numbers and frequencies listed in Table 1, where r and f_r are the mode number and frequency of the exciting force wave respectively. The discussion about the components of $P_{ef}(\theta,t)$ given in Table 1 is as follows:

- 1^{st} group of double frequency force wave is formed by the multiplication of the main pole of the excitation fields and identical order numbers of the field waves. Therein the fundamental force wave with double fundamental frequency is uninteresting from the acoustical point of view. However, the force wave with double fundamental frequency must be considered in the vibration calculation. The harmonic force waves are not of interest in terms of acoustics and vibrations because the mode number of the force waves is high and amplitude is negligibly small.
- 2^{nd} group of harmonic force wave is formed by the cross multiplication of the harmonics of the excitation fields and different order numbers of the field waves.
- 3^{rd} group of harmonic force wave is produced by the multiplication of the additional slotting permeance fields and identical order numbers of the field waves.
- 4^{th} group of harmonic force wave is formed by the multiplication of the additional slotting permeance fields and different order numbers of the field waves.
- 5^{th} group of harmonic force wave is formed by the multiplication of the main pole field of the excitation field and the additional slotting permeance fields, which is actually one of the main origins for acoustic noise and vibrations.
- 6^{th} group of harmonic force wave is produced by the multiplication of the armature field and the main pole field of the excitation field.
- 7^{th} group of harmonic force wave is formed by the multiplication of the armature field and by the additional slotting permeance fields.
- 8^{th} group of double fundamental frequency force wave is formed by the multiplication of the armature fields and identical order numbers of the field waves. This group is also one of the main origins for the acoustic noise and vibrations.
- 9^{th} group of double fundamental frequency force wave is produced by the multiplication of the armature fields and different order numbers of the field waves.

The effects of vibration and noise produced by the exciting force waves are proportional to the amplitude of the exciting force. On the other hand, these effects depend on the values of the mode number and frequency of the exciting force waves. Table 2 shows the vibration displacement in the machine core circumference as a function of mode number. It can be noted that smaller the value of mode number, larger the distance between neighboring nodes of the stator core bending and distortion. The stator core distortion in this case becomes large. Usually, when the stator core vibrates, the amplitude of dynamic distortion is approximately inversely proportional to the fourth power of the mode number value.

IV. MACHINE VIBRATION MODES

The exciting force acting on the cores of the stator and rotor, and the mechanical vibration forces acting on the bearings, may produce troublesome noise and vibration. This is particularly the case of when the frequencies of the exciting forces for important mode numbers are equal to or near to the natural frequencies of the machine. So machine sizing must assess the natural frequencies of the stator so that appropriate structural sizing can be arranged to give a mismatch of the frequencies of the important exciting force waves and the natural frequencies of the machine.

Although the exciting forces are exerted on the stator teeth, the vibration amplitude is much smaller than the amplitude of vibration of the stator core. The stator is of double–ring type, consisting of an outer frame and an inner stator core. The frame is linked to the core laminations by ribs or keys. An analytical method is presented here for the calculation of the natural frequencies, which concentrates on the natural vibration modes of the stator. In predicting the natural vibration frequencies, it was assumed that the stator core is a round rigid body. And the teeth and winding have no rigidity, so that their mass is attached to the core. It was also assumed that the only effect of the all defects and notches (such as ducts) is a reduction in the mass. In addition, the periodic force waves with mode number are symmetrically exerted on the stator core ring, and a damping factor will be considered to account for damping effects.

The following formulas are used to predict the ideal natural vibration frequencies of the radial flux machines for the force wave with mode number [5-9],

$$f_{0r} = \frac{1}{2\pi}\sqrt{\frac{k_{r-core} + k_{r-frame}}{m_{r-core} + m_{r-frame}}} \quad \text{[Hz]} \qquad (20)$$

where $k_{r\text{-}core}$ is the equivalent spring stiffness of the stator core including stator windings and teeth, $k_{r\text{-}frame}$ is the equivalent spring stiffness of the stator frame, $m_{r\text{-}core}$ is the stator core mass including stator windings and teeth, $m_{r\text{-}frame}$ is the stator frame mass.

The stator core mass and the stator frame mass are found to be [5-9]

$$m_{r-core} = \begin{cases} G_{core} & r = 0 \\ G_{core}\dfrac{r^2+1}{r^2} & r \ge 2 \end{cases} \quad \text{[kg]} \qquad (21)$$

$$m_{r-frame} = \begin{cases} G_{frame} & r = 0 \\ G_{frame}\dfrac{r^2+1}{r^2} & r > 2 \end{cases} \quad \text{[kg]} \qquad (22)$$

where G_{core} is the stator core weight including stator windings and teeth, G_{framee} is the stator frame weight.

The equivalent spring stiffness of the stator core and the stator frame are expressed as [5-9]

$$k_{r-core} = \begin{cases} \dfrac{2\pi E_{core} h_{core} L_{core}}{R_{ac-core}} F_{r-core}^2 & r = 0 \\ \dfrac{2\pi E_{core} h_{core}{}^3 L_{core}}{12 R_{av-core}^3} (r^2-1)^2 F_{r-core}^2 & r \ge 2 \end{cases} \quad \text{[N/m]} \qquad (23)$$

$$k_{r-frame} = \begin{cases} \dfrac{2\pi E_{frame} h_{frame} L_{frame}}{R_{ac-frame}} F_{r-frame}^2 & r = 0 \\ \dfrac{2\pi E_{frame} h_{frame}{}^3 L_{frame}}{12 R_{av-frame}^3} (r^2-1)^2 F_{r-frame}^2 & r \ge 2 \end{cases} \quad \text{[N/m]} \qquad (24)$$

where E_{core} is the Young's modulus of elasticity for the stator core, E_{frame} is the Young's modulus of elasticity for stator frame, h_{core} is the height of the stator core, h_{frame} is the height of the stator frame, L_{core} is the length of the stator core, L_{frame} is the length of the stator frame, $R_{av\text{-}core}$ is the average radius of the stator core, $R_{av\text{-}framee}$ is the average radius of the stator frame, $F_{r\text{-}core}$ is the damping factor of the stator core, $F_{r\text{-}framee}$ is the damping factor of the stator frame.

According as mechanical impedance method theory, the vibration displacement of the machine of the mode number and frequency concerned can be derived as

$$Y_{r/f_r} = \begin{cases} \dfrac{P_{eq-r/f_r}}{(k_{r-core}+k_{r-frame}) - \omega_r^2 (m_{r-core}+m_{r-frame})} \\ \dfrac{P_{eq-r/f_r}}{k_{r-core-rotor} - \omega_r^2 m_{r-core-rotor}} \\ \dfrac{P_{eq-r/f_r}}{k_{r-core-stator} - \omega_r^2 m_{r-core-stator}} \end{cases} \qquad (25)$$

where P_{eq-r/f_r} is the equivalent exciting force in the stator inner surface of the mode number and frequency concerned, ω_r is the radian frequency of the exciting force waves, $k_{r-core-rotor}$ is the equivalent spring stiffness of the external rotor core including rotor PM for axial flux external rotor (Torus) topologies, $k_{r-core-stator}$ is the equivalent spring stiffness of the external stator core including stator windings and teeth for the axial flux internal rotor topology machines.

The equivalent exciting force in the airgap surface for the mode number and frequency concerned is

$$P_{eq-r/f_r} = S_g\, P_{peak-r/f_r} \qquad (26)$$

where P_{peak-r/f_r} is the amplitude of the exciting force waves for the mode number and frequency concerned. The airgap surface area is

$$S_g = \begin{cases} \pi D_g L_{eff} & \text{For radial flux topologies} \\ \dfrac{\pi}{4}(D_0^2 - D_i^2) & \text{For axial flux topologies} \end{cases} \quad (27)$$

The amplitude of the vibrating velocity of the machine is given by

$$V_{pk-r} = \omega_r Y_{pk-r} \quad (28)$$

where Y_{pk-r} is the amplitude of the particle vibratory displacement.

V. RESULTANT SOUND POWER LEVEL

The surface vibration of machines due to the exciting force waves is regarded as a series of rotating sinusoidal waves of displacement from Equations (19) and (25). Yang's (1975) equation of the sound power for the cylindrical sound wave model is [10]

$$W_{Cylin-r} = 2\rho C\pi^2 f_r^2 Y_{pk-r}^2 S_{Cylin} I_{re-r} \quad (29)$$

where ρ is the density of the medium (for air ρ=1.186 kg/m^3), f_r is the frequency of the sound wave, C is the traveling speed of sound in the medium (for air, C =344 m/s), S_{Cylin} is the surface vibration area for the radial flux cylindrical machine which is perpendicular to the direction of travel of sound and I_{re-r} is the relative sound intensity coefficient.

The sound power for the plane sound wave model can be expressed as [1]

$$W_{plane-r} = 2\rho C\pi^2 f_r^2 Y_{pk-r}^2 S_{plane} I_{re-r} \quad (30)$$

where S_{Plane} is the surface vibration area for the axial flux disc machines and this area is perpendicular to the direction of the travel of sound. Finally the resultant sound power level in dB is defined as

$$L_{Wt} = \sum_{i=1}^{n} L_{Wi} = 10\log\left[\sum_{i=1}^{n} \frac{W_i}{W_0}\right] = 10\log\left[\sum_{i=1}^{n} 10^{0.1L_{Wi}}\right] \quad (31)$$

where $L_{Wi} = 10\log\dfrac{W_i}{W_0}$ [dB], W_i is the sound power [w], $W_0 = 10^{-12}$ [w] is the reference value of the sound power.

VI. MINIMIZATION OF RESULTANT SOUND POWER LEVEL FOR 200HP RADIAL FLUX SLOTTED SURFACE MOUNTED PM MACHINE

Inspecting Equations (10), (17) and (19), one can realize that optimal design for stator winding, PM rotor shape and PM rotor skew angle are based on the minimization of resultant sound power level for low noise motor design. Particularly skewing rotor PM has a strong effect on reducing resultant sound power level. On the other hand, according to mechanical vibration theory and Equations (20)-(25) one can understand that the choice of the stator frame height is crucial for reducing the vibration.

A) Noise and Vibration vs. Skew Angle

The resultant sound power level and maximum vibration velocity plots are shown in Figures 1 and 2 respectively for full load condition. As can be seen from Figure 1 the resultant sound power level is minimum at a skew angle of 34.56 degrees. Figures 3 and 4 illustrate the resultant sound power level and vibration velocity plots for the no load condition. The resultant sound power level for the no load condition is minimum for an electrical skew angle of 33.6 degrees. A summary of the results is given in Table 3.

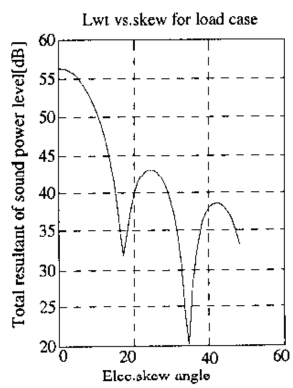

Fig 1. Resultant sound power level vs skew angle for full-load case

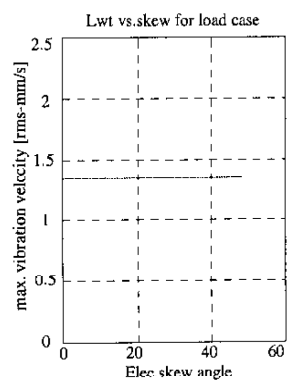

Fig 2. Maximum vibration velocity vs. skew angle for full-load case

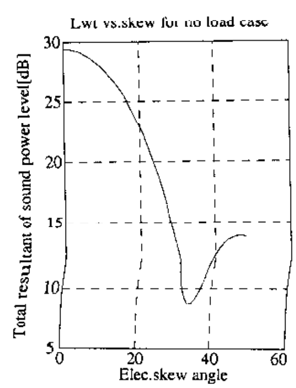

Fig 3. Resultant sound power level vs. skew angle for no-load case

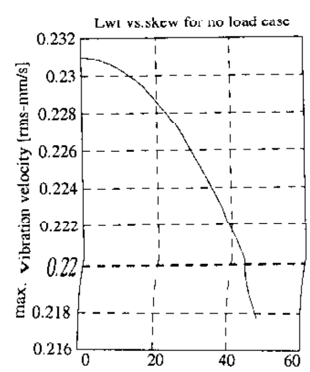

Fig 4. Maximum vibration velocity vs. skew angle for no-load case

Table 3. Minimum resultant sound power level and optimum skew angle for no load and full load conditions

	No load	Full load
Resultant sound power level [dB]	8.8 dB	20.14 dB
Optimum skew angle [deg]	33.6 degrees	34.56 degrees

B) Noise and Vibration vs. Height of Stator Frame

Noise and vibration analysis have been carried out for different frame thickness. Figures 5 to 8 show resultant sound power level and maximum vibration velocity for full load and no load conditions as a function of the stator frame thickness. It should be noted that skewing the rotor magnets is essential for reducing the sound power level while choosing the stator frame thickness is significant for reducing the machine vibration. As can be seen from the analysis, the minimum resultant sound power level occurs at 17.92 dB and the optimum stator frame thickness for this situation is 3.5 cm (1.38 inches) for full load conditions.

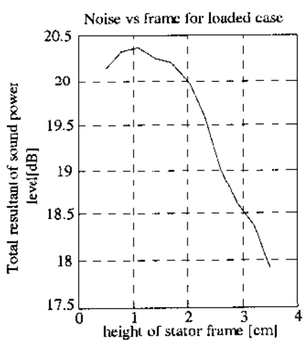

Fig 5. Resultant sound power level vs. height of stator frame for full-load case

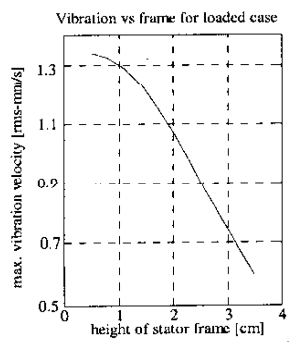

Fig 6. Maximum vibration velocity vs. height of stator frame for full-load case

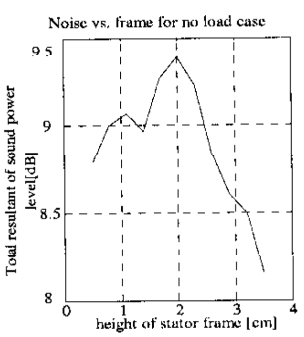

Fig 7. Resultant sound power level vs. height of stator frame for no load case

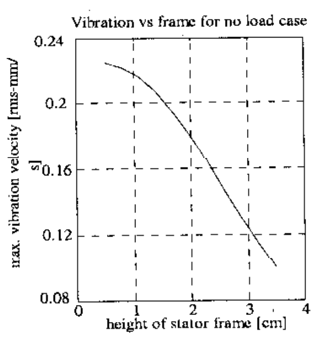

Fig 8. Maximum vibration velocity vs. height of stator frame for no load case

VII. COMPARISON OF NON-SLOTTED AND SLOTTED AXIAL AND RADIAL FLUX SURFACE MOUNTED PERMANENT MAGNET TYPE MACHINES

A detailed noise and vibration analysis was obtained for slotted and non-slotted radial flux (RFSM-S and RFSM-NS), double rotor disc type axial flux (TORUS-S and TORUS-NS) and axial flux internal rotor (AFIR-S and AFIR-NS) surface mounted PM machines. The resultant sound power levels, maximum vibration velocities and maximum vibration displacement of main vibration source values are shown in Figure 9 through Figure 14. It should be noted that both high and low frequency ranges of vibration exist in any machine. The high frequency range of vibration is the main source of acoustics compared to low frequency range of vibration and causes the main acoustic noise that is in the range of the human ear. However, the low frequency range of vibration is the main vibration source compared to high frequency vibration. Skewing reduces the high frequency noise. As the thickness of the frame and core increase, the equivalent spring stiffness increases and results in reduced the low frequency vibration.

Non Skewed Rotor PM – Full-load Case

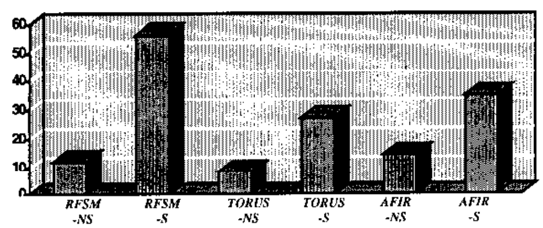

Fig 9. Resultant sound power level (L_{wr}) [dB]

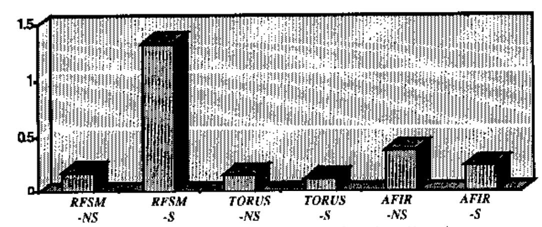

Fig 10. Maximum vibration velocity of main vibration source (*Vel_max*) [rms-mm/s]

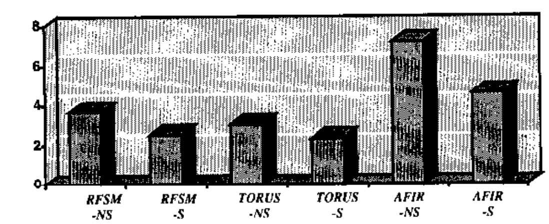

Fig 11. Maximum vibration displacement of main vibration source (*Y_max*) [peak-mm/s]

Skewed Rotor PM – Full-load Case

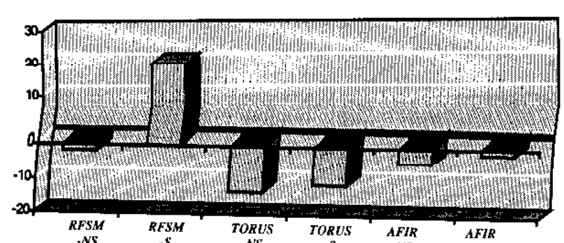

Fig 12. Resultant sound power level (L_{wr}) [dB]

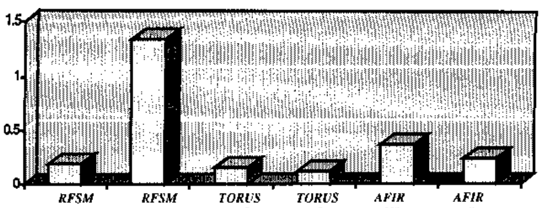

Fig 13. Maximum vibration velocity of main vibration source (*Vel_max*) [rms-mm/s]

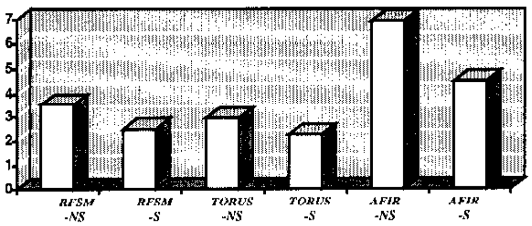

Fig 14. Maximum vibration displacement of main vibration source (*Y_max*) [peak-mm/s]

From this information and data gathered, following conclusions can be obtained:

- In general, non-slotted topologies have the lower sound power levels than slotted topologies. In particular, the non-slotted TORUS topology has the lowest sound power level.
- Skewed rotor magnets reduce the noise level and high frequency vibration.
- TORUS-S machine has the highest spring stiffness and lowest vibration displacement.
- TORUS-NS machine has the lowest noise level and lower vibration displacement.
- The conventional radial flux slotted PM machine has the highest noise and vibration level compared to its non-slotted counterpart and axial flux topologies.

VIII. CONCLUSIONS

Analysis of electromagnetic vibration and noise assessment and methods to minimize resultant sound power level for low noise motor design has been presented in the paper. The approach synthesizes the analysis of electromagnetic exciting force, mechanical vibration and sound radiation. The linear model of the exciting force wave has been formulated in terms of liner model of the air gap resultant field and the air gap permeance wave, which should be useful to optimum design of stator winding, PM rotor shape and PM rotor skew angle for minimization of resultant sound power level for low noise motor design. Mode number and frequency of the exciting force wave and vibration displacement should be used to predict the spectrum and dominant components of the noise and vibration as well as the natural frequency in terms of the geometry of the machine and elasticity modulus of the machine components. In the meantime, the resultant sound power level, maximum vibration velocity of main vibration source and maximum vibration displacement of the main vibration source are introduced as main performance of electromagnetic vibration and noise assessment of electrical machines. Moreover, skewing rotor PM has a strong effect on reducing resultant sound power level and choosing the stator frame height is crucial for reducing the vibration.

In addition, the sound power for the cylindrical sound wave model and the sound power for the plane sound wave model are introduced in order to evaluate the acoustic noise radiation of both axial flux and radial flux machines respectively. Electromagnetic vibration and acoustic noise assessment of both axial flux and radial flux surface mounted motor structures (Torus, axial flux internal rotor (AFIR) and radial flux machines) are completed.

IX. ACKNOWLEDGMENTS

The authors are grateful to the Naval Surface Warfare Center for their financial support (Grant Number: N00014-98-1-0807).

X. REFERENCES

[1] T. A. Lipo, S. Huang and M. Aydin, "Performance assessment of axial flux permanent magnet motors for low noise applications", Final Report to Office of Naval Research, Oct 2000.

[2] S Huang, M. Aydin and T. A. Lipo, "Comparison of (non-slotted and slotted) surface mounted PM motors and axial flux motors for submarine ship drives", Third Naval Symposium on Electrical Machines, Philadelphia, Dec. 2000.

[3] S Huang, M. Aydin and T. A. Lipo, "A direct approach to electrical machine performance evaluation: Part-1: Torque density assessment and sizing optimization", 2001 IEEE-IAS 36th Annual Meeting (pending)

[4] S Huang, M. Aydin and T. A. Lipo, "A Direct approach to Electrical machine performance evaluation: Part-2: Torque quality assessment", 2001 IEEE-IAS 36th Annual Meeting (pending)

[5] Y. Chen, Z. Zhu and S. Ying, "Analysis and Control of Noise of Electrical Machines", China: Zhejiang University Press. 1987.

[6] S. Chen, "Electrical Machinery Design", Beijing, China, Machinery Industry Press, 1982.

[7] A.Ellison, S. Yang, "Natural frequencies of stators of small electric machines", IEE, Proc. Vol.118 (I), 1971, pp. 185-190.

[8] E. Erdelyi, G. Horvay, "Vibration modes of stators of induction motors," ASME Transaction, Vol.24 (E), 1957, pp. 39-45.

[9] W. Cai and P. Pillay, "Resonance frequencies and mode shapes of switched reluctance motors," IEEE International Electrical Machines and Drives Conference, IEMDC 1999, Seattle, pp. 44-47.

[10] S.J. Yang, "Low-Noise Electrical Motors", Clarendon Press, Oxford, 1981.

[11] P.L. Belmans, "Noise and Vibrations of Electrical Machines", Elsevier, Amsterdam/New York, 1989.

[12] P. Vijiayaghavan and R.Krishnan, "Noise in electric machines: A review," IEEE Industry Applications Society Annual Meeting, 1998, St. Louis, USA, pp. 251-258.

X. BIOGRAPHIES

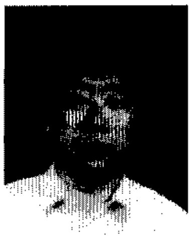

Surong Huang was born in Shanghai, China, in 1953. He graduated from Shanghai University of Technology, Shanghai, China, in 1977. In 1977, he joined the Shanghai University of Technology, Shanghai, China, as an Instructor Associate. He was promoted to Lecturer and Associate Professor at Shanghai University in 1987 and 1993, respectively. He was a Visiting Faculty Member in the Department of Electrical and Computer Engineering, University of Wisconsin- Madison in 1995-1996 and 1998-2000. He is engaged in research and development of new types of electrical machines and drive systems. His interests include design, control, and modeling of electrical machines and AC drives, vibration and noise analysis of electrical machines. He has published more than forty papers on these topics.

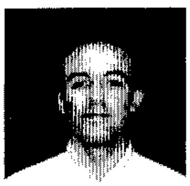

Metin Aydin, a native of Turkey, received his B.S. degree in Electrical Engineering from Istanbul Technical University (ITU), Turkey, in 1993 and his M.S. degree in Electrical Engineering from the University of Wisconsin-Madison, WI, in 1997. He is presently a research assistant with WEMPEC (Wisconsin Electrical Machines and Power Electronics Consortium) and a Ph.D. student in Electrical Engineering at University of Wisconsin-Madison. His research interests include electrical machine design, particularly brushless permanent magnet machine design and control, electric drives, modeling and simulation. He is also a student member of IEEE and the vice president of the ITU Alumni Wisconsin Branch.

Thomas A. Lipo is (M'64-SM'71-F'87) is a native of Milwaukee, WI. From 1969 to 1979, he was an Electrical Engineer in the Power Electronics Laboratory, Corporate Research and Development, General Electric Company, Schenectady NY. He became a Professor of electrical engineering at Purdue University, West Lafayette, IN, in 1979 and, in 1981, he joined the University of Wisconsin, Madison, in the same capacity, where he is presently the W. W. Grainger Professor for power electronics and electrical machines.

Dr. Lipo has received the Outstanding Achievement Award from the IEEE Industry Applications Society, the William E. Newell Award of the IEEE Power Electronics Society, and the 1995 Nicola Tesla IEEE Field Award from the IEEE Power Engineering Society for his work. Over the past 35 years, he has served the IEEE in numerous capacities, including President of the IEEE Industry Applications Society.

XI. APPENDIX

Table 1. Main parameters of the exciting force waves

Group	Exciting force waves equation	Amplitude P_{peak-r,f_r}	Mode number r	Frequency f_r
1st	$p_{1^{st}} = \sum_{\mu} \frac{B_{\mu}^2 \overline{\Lambda}_0^2}{4\mu_0} \cos(2\mu\omega_1 t - 2\mu p\theta)$	$(B_{\mu}\overline{\Lambda}_0)^2/(4\mu_0)$	$r = 2\mu p$	$f_r = 2\mu f_1$
2nd	$p_{2^{nd}} = \frac{1}{2\mu_0} \sum_{\mu_1} \sum_{\mu_2 (\mu_2 > \mu_1)} B_{\mu_1} B_{\mu_2} \overline{\Lambda}_0^2 \cos[(\mu_2 \pm \mu_1)\omega_1 t - (\mu_2 \pm \mu_1)p\theta]$	$(B_{\mu_1}\overline{\Lambda}_0)(B_{\mu_2}\overline{\Lambda}_0)/(2\mu_0)$ $(\mu_2 > \mu_1)$	$r = (\mu_2 + \mu_1)p$ $r = (\mu_2 - \mu_1)p$	$f_r = (\mu_2 + \mu_1)f_1$ $f_r = (\mu_2 - \mu_1)f_1$
3rd	$p_{3^{rd}} = \sum_{\mu} \sum_{k} \frac{1}{16\mu_0} B_{\mu}^2 \overline{\Lambda}_k^2 \cos[2\mu\omega_1 t - 2(\mu p \pm kZ_s)\theta]$	$(B_{\mu}\overline{\Lambda}_k)^2/(16\mu_0)$	$r = 2(\mu p + kZ_s)$ $r = 2(\mu p - kZ_s)$	$f_r = 2\mu f_1$ $f_r = 2\mu f_1$
4th	$p_{4^{th}} = \sum_{\mu_1} \sum_{\mu_2 (\mu_2 > \mu_1)} \sum_{k_1} \sum_{k_2 (k_2 > k_1)} (-1)^{k_1+k_2} \frac{1}{8\mu_0} B_{\mu_1} B_{\mu_2} \overline{\Lambda}_{k_1} \overline{\Lambda}_{k_2}$ $\cos\{(\mu_2 \pm \mu_1)\omega_1 t - [(\mu_2 \pm \mu_1)p \pm (k_2 \pm k_1)Z_s]\theta\}$	$(B_{\mu_1}\overline{\Lambda}_{k_1})(B_{\mu_2}\overline{\Lambda}_{k_2})/(8\mu_0)$; $(\mu_2 > \mu_1,\ k_2 > k_1)$	$r = (\mu_2 + \mu_1)p + (k_2 + k_1)Z_s$ $r = (\mu_2 + \mu_1)p + (k_2 - k_1)Z_s$ $r = (\mu_2 + \mu_1)p - (k_2 + k_1)Z_s$ $r = (\mu_2 + \mu_1)p - (k_2 - k_1)Z_s$ $r = (\mu_2 - \mu_1)p + (k_2 + k_1)Z_s$ $r = (\mu_2 - \mu_1)p + (k_2 - k_1)Z_s$ $r = (\mu_2 - \mu_1)p - (k_2 + k_1)Z_s$ $r = (\mu_2 - \mu_1)p - (k_2 - k_1)Z_s$	$f_r = (\mu_2 + \mu_1)f_1$ $f_r = (\mu_2 + \mu_1)f_1$ $f_r = (\mu_2 + \mu_1)f_1$ $f_r = (\mu_2 + \mu_1)f_1$ $f_r = (\mu_2 - \mu_1)f_1$ $f_r = (\mu_2 - \mu_1)f_1$ $f_r = (\mu_2 - \mu_1)f_1$ $f_r = (\mu_2 - \mu_1)f_1$
5th	$p_{5^{th}} = \sum_{\mu_1} \sum_{\mu_2} \sum_{k} (-1)^{k+1} \frac{1}{4\mu_0} B_{\mu_1} B_{\mu_2} \overline{\Lambda}_0 \overline{\Lambda}_k$ $\cos\{(\mu_2 \pm \mu_1)\omega_1 t - [(\mu_2 \pm \mu_1)p \pm kZ_s]\theta\}$	$(B_{\mu_2}\overline{\Lambda}_0)(B_{\mu_1}\overline{\Lambda}_k)/(4\mu_0)$	$r = (\mu_2 + \mu_1)p + kZ_s$ $r = (\mu_2 + \mu_1)p - kZ_s$ $r = (\mu_2 - \mu_1)p + kZ_s$ $r = (\mu_2 - \mu_1)p - kZ_s$	$f_r = (\mu_2 + \mu_1)f_1$ $f_r = (\mu_2 + \mu_1)f_1$ $f_r = (\mu_2 - \mu_1)f_1$ $f_r = (\mu_2 - \mu_1)f_1$
6th	$p_{6^{th}} = \frac{1}{2\mu_0} \sum_{\nu} \sum_{\mu} B_{\mu} B_{\nu} \overline{\Lambda}_0 \cos[(\mu \pm 1)\omega_1 t - (\mu \pm \nu)p\theta - (\pm\psi + \frac{\pi}{2})]$	$B_{\nu} B_{\mu} \overline{\Lambda}_0/(2\mu_0)$	$r = (\mu + \nu)p$ $r = (\mu - \nu)p$	$f_r = (\mu + 1)f_1$ $f_r = (\mu - 1)f_1$
7th	$p_{7^{th}} = \sum_{\nu} \sum_{\mu} \sum_{k} (-1)^{k+1} \frac{1}{4\mu_0} B_{\nu} B_{\mu} \overline{\Lambda}_k$ $\cos\{(\mu \pm 1)\omega_1 t - [(\mu p \pm kZ_s) \pm \nu p]\theta - (\pm\psi \pm \frac{\pi}{2})\}$	$B_{\nu} B_{\mu} \overline{\Lambda}_k/(4\mu_0)$	$r = \mu p + kZ_s + \nu p$ $r = \mu p - kZ_s + \nu p$ $r = \mu p + kZ_s - \nu p$ $r = \mu p - kZ_s - \nu p$	$f_r = (\mu + 1)f_1$ $f_r = (\mu + 1)f_1$ $f_r = (\mu - 1)f_1$ $f_r = (\mu - 1)f_1$
8th	$p_{8^{th}} = \sum_{\nu} \frac{B_{\nu}^2}{4\mu_0} \cos[2\omega_1 t - 2\nu p\theta - 2(\psi + \frac{\pi}{2})]$	$B_{\nu}^2/(4\mu_0)$	$r = 2\nu p$	$f_r = 2f_1$
9th	$p_{9^{th}} = \frac{1}{2\mu_0} \sum_{\nu_1} \sum_{\nu_2 (\nu_2 > \nu_1)} B_{\nu_1} B_{\nu_2} \cos[2\omega_1 t - (\nu_1 + \nu_2)p\theta - 2(\psi + \frac{\pi}{2})]$	$B_{\nu_1} B_{\nu_2}/(2\mu_0)$ $(\nu_2 > \nu_1)$	$r = (\nu_1 + \nu_2)p$	$f_r = 2f_1$

r — mode number of the exciting force waves, f_r — frequency of the exciting force waves, P_{peak-r,f_r} — amplitude of the exciting force waves.

Table 2. Vibration displacement in the machine core circumference for different mode number

	r = 0	R − 1	r = 2	r = 3	r = 4	r = 5
Radial Flux PM Machine	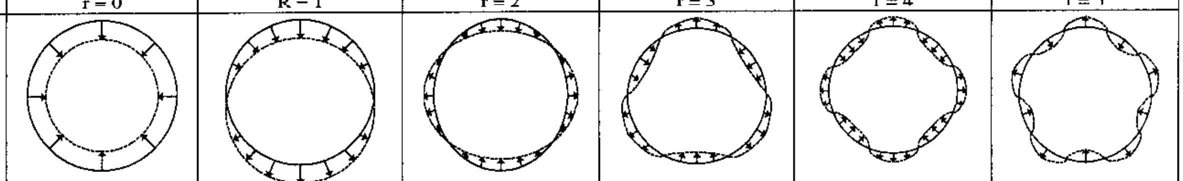					
TORUS Type Machine	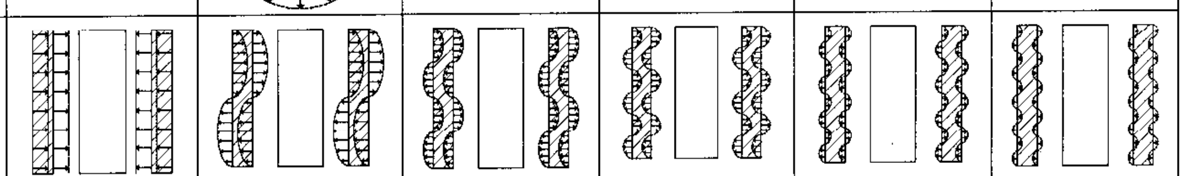					
AFIR Type Machine	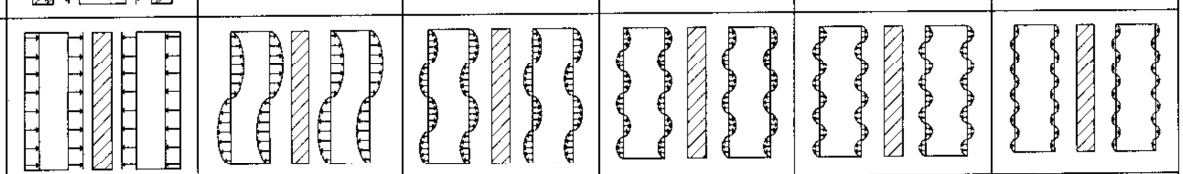					
Exciting force wave in airgap circumference